Physics From Deep Virtual Exclusive Data

Charles Hyde

OLD DOMINION UNIVERSITY

A few starting thoughts

- Our analysis methods could probably be improved
- Most experiments analyzed by binning data, and then fitting distributions
- Possibilities to use Maximum Likelihood methods on un-binned data
  - Very computationally intensive
  - Opportunities for AI/ML?

Radiative Corrections

- Higher order in $\alpha_{QED} \approx 1/137$
  - Not small! Parametrically $\frac{\alpha_{QED}}{\pi}\ln[Q^2/m_e^2]$~0.1
  - Radiation of soft photons
  - Virtual photon loop coupling across *(e,e')* vertex
  - Vacuum polarization: e^+e^- loop in virtual photon propagator
- Must be incorporated into experimental analysis
- More on DVCS Radiative Corrections later.

Electroproduction

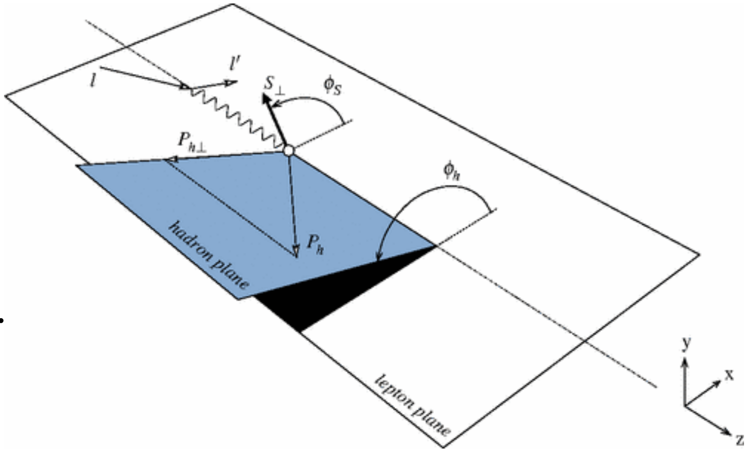

- "Trento Convention" for ϕ_h
  - A. Bacchetta, et al., Phys.Rev.D**70**, 117504 (2004).
- (e,e'h)X
  - *D. Drechsel and L. Tiator, J. Phys. G 18, 449 (1992).*
  - $\frac{d^5\sigma}{d\Omega dk' dt d\phi_h} = \frac{d^3\Gamma}{d\Omega dk'}\Big[\frac{d\sigma_T}{dt} + \epsilon\frac{d\sigma_L}{dt} + \sqrt{2\epsilon(1+\epsilon)}\cos\phi_h \frac{d\sigma_{TL}}{dt} + \epsilon\cos(2\phi_h)\frac{d\sigma_{TT}}{dt} + h\sqrt{2\epsilon(1+\epsilon)}\sin\phi_h\frac{d\sigma_{TL'}}{dt}\Big]$
  - $d\Gamma =$ "Virtual Photon Flux" *L. N. Hand, Phys. Rev.* ***129****, 1834 (1963).*
- Vector Meson Production : K.Schillilng, G.Wolf, *Nucl.Phys.B* **61** (1973) 381-413
  - Analyze the decay angular distribution *e.g.* $\boldsymbol{\phi} \to K^+ K^-$
  - Extract polarization density matrix of phi-meson (about 28 terms!)
  - R4_00 term: L→L polarization➔ $d\sigma_L$
  - QCD factorization predicts dominance of $d\sigma_L$ over $d\sigma_T$ for **light** mesons

Vector Meson Electroproduction

- K.Schillilng, G.Wolf, *Nucl.Phys.B* **61** (1973) 381-413
- Example: two-body decay of vector-meson production $(e, e'\phi \to K^+K^-)$
  - Analyze the decay angular distribution *e.g.* $\boldsymbol{\phi} \to K^+ K^-$ or $\rho \to \pi^+\pi^-$
  - Extract polarization density matrix of vector-meson
    - Decay angular distribution of Wigner d-functions of J =0,1,2 ➔ 20 structure functions!

$$r_{00}^{04} \quad \text{from } \cos(2\theta) \text{ term in polar decay-angle distribution}$$

$$R = \frac{\sigma_L}{\sigma_T} = \frac{1}{\epsilon}\frac{r_{00}^{04}}{(1-r_{00}^{04})}, \qquad \text{SCHC}$$

Exclusive Vector Meson Production at HERA

- Summary talk from Diffraction2004
  A. Levy / Nuclear Physics B (Proc. Suppl.) **146** *(2005) 92–101, arXiv:0501008*
- Ratio grows slower than Q^2
  - Factorization of σ_L and σ_T can be considered separately

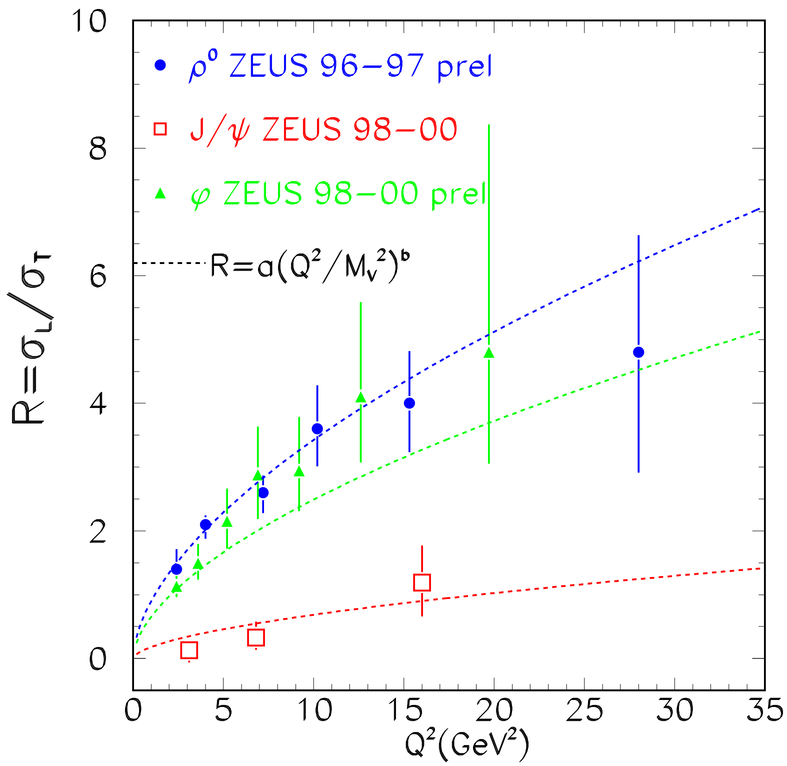

Vector Meson production: *t*-dependence

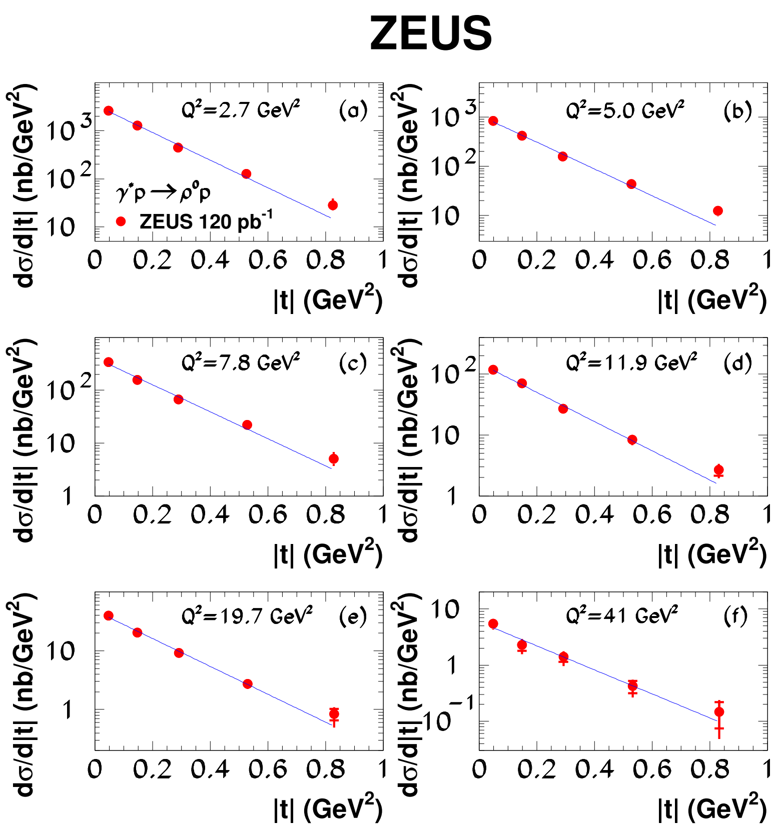

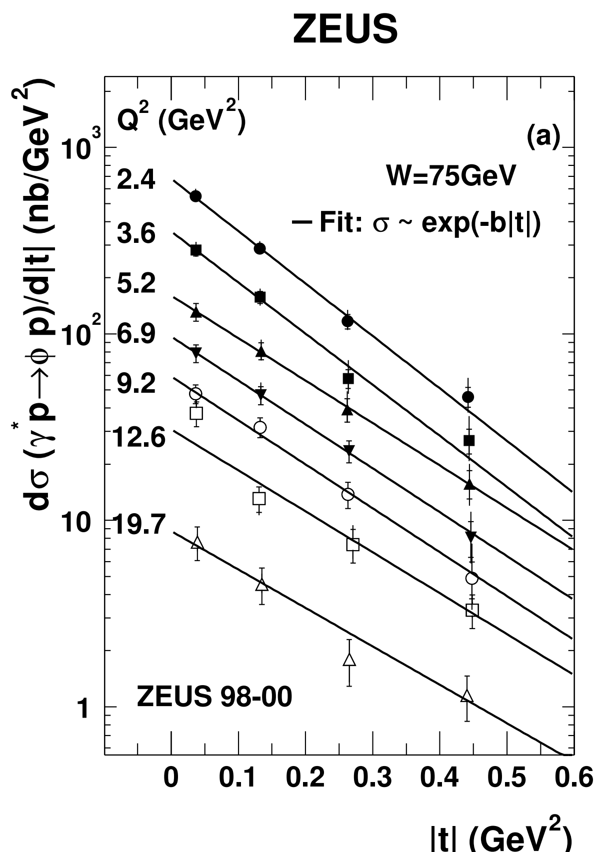

G.Wolf
https://arxiv.org/abs/0907.1217

Exclusive Vector Meson Production at HERA

G.Wolf https://arxiv.org/abs/0907.1217

- Naïve interpretation:
  Slope parameter represents convolution of `meson size' with nucleon size
  - Meson 'size' ~ $1/\sqrt{Q^2 + M_V^2}$
  - Nucleon size ~ intrinsic
- HERA data mostly interpreted in the $q\bar{q}$ dipole picture, rather than GPDs

zDESY-07-118_11

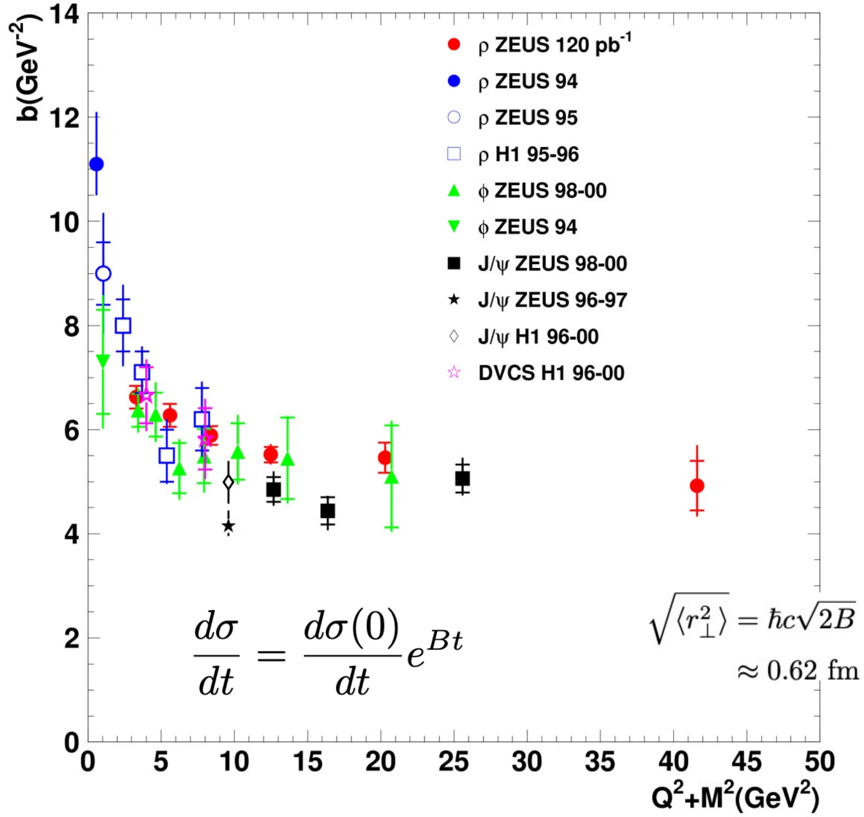

Deep Virtual π^0 and η Production

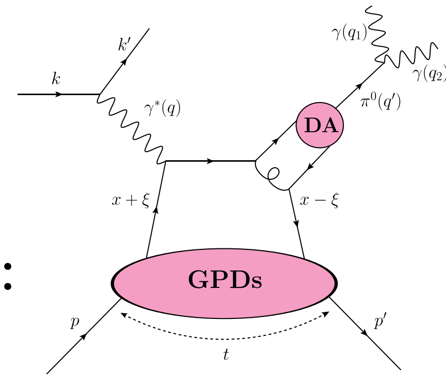

Invariants

$Q^2 = -(k-k')^2$

$x_B = \frac{Q^2}{2q \cdot p}$

$W^2 = (q+p)^2$

$y = \frac{q \cdot p}{k \cdot p}$

$t = (q-q')^2$

$t' = t_{\min} - t$

- Naïve QCD Factorization, asymptotic behavior:
  - $d\sigma_L \sim 1/Q^6$,
  - $d\sigma_T \sim 1/Q^8$
- Initial Hall A / CLAS experiments suggested $d\sigma_T$ dominant at $Q^2 \leq 2$ GeV^2
  - S. Ahmad, G. R. Goldstein and S. Liuti, Phys. Rev. D **79**, 054014 (2009)
    - Helicity flips via $\sigma^{\mu\nu}$ operator at π^0 and N vertices→nominally suppressed by $\sqrt{\Lambda^2/Q^2}$
  - S. V. Goloskokov and P. Kroll, Eur.Phys.J.A **47**, 112 (2011),
    - "Generalized Perturbative Approach", account for "finite-size" of meson vertex
  - Chiral Symmetry breaking leads to strong helicity flip pseudo-scalar distribution amplitude (DA): $q\bar{q} \to \pi^0, \eta$

Hall-A Rosenbluth Separation: H($e,e'\pi^0$)p

- M.Defurne, *et al.*, PRL **117**, 262001 (2016)
  - $\langle x_B \rangle = 0.36$, $Q^2 = 1.5, 1.75, 2.0$ GeV^2

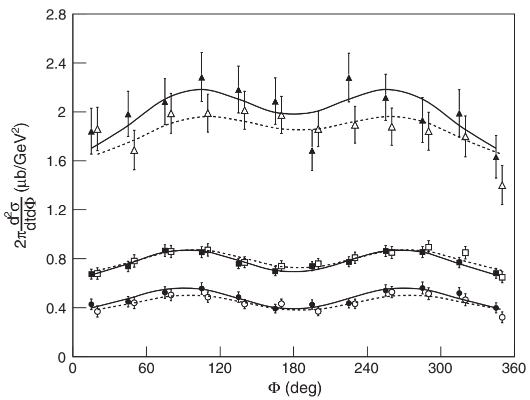

FIG. 3. $2\pi(d^2\sigma/dtd\phi)$ for $Q^2 = 1.5$ (triangles), 1.75 (squares), and 2 GeV^2 (circles) at $x_B = 0.36$ and $t_{\min} - t = 0.025$ GeV^2. The cross sections extracted at low (high) ϵ are shown in open (solid) symbols [and dashed (solid) lines].

Long Dashed:
Goldstein, Hernandez, Liuti, Phys. Rev. D **84**, 034007 (2011).
Solid:
S. Goloskokov and P. Kroll, Eur. Phys. J. A **47**, 112 (2011).

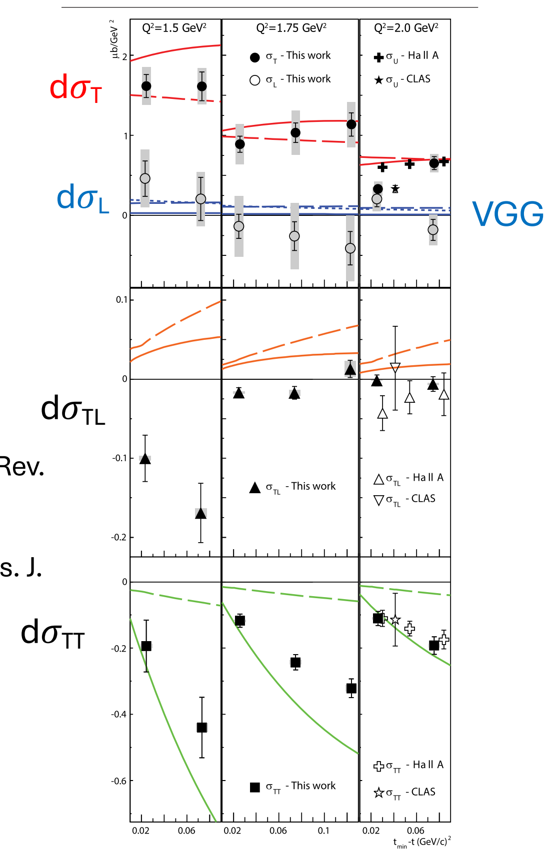

FIG. 4. $d\sigma_T$ (full circles), $d\sigma_L$ (open circles), $d\sigma_{TL}$ (triangles), and $d\sigma_{TT}$ (squares) as a function of $t_{\min} - t$ for $Q^2 = 1.5$ (left), 1.75 (center), and 2 GeV^2 (right) at $x_B = 0.36$. The full lines are predictions from Ref. [16] and the long-dashed lines from Ref. [25]. The short-dashed line show the VGG model [2] for $d\sigma_L$. Solid boxes around the points show normalization systematic uncertainties; for $d\sigma_L$ and $d\sigma_T$, these uncertainties are strongly anticorrelated. Previous unseparated measurements ($\sigma_U = \sigma_T + \epsilon\sigma_L$) at similar, but not equal, kinematics are also shown and described in the text.

Transversity GPDs

- Light cone matrix elements of $\sigma^{\mu\nu}$
  - Tensor charge is a `macroscopic' property of the nucleon
  - S. Ahmad, G. R. Goldstein and S. Liuti, Phys. Rev. D **79**, 054014 (2009)
- Combined analysis of π^0 dσ_T, p & n ➔
  - $\langle x_B \rangle = 0.36$, $Q^2 = 1.75$ GeV^2
  - Systematic errors can be reduced with inclusion of CLAS η data
    - Resolve signs of GPD$_T$

M.Mazouz et al., [Hall A]
PRL **118,** 222002 (2017)

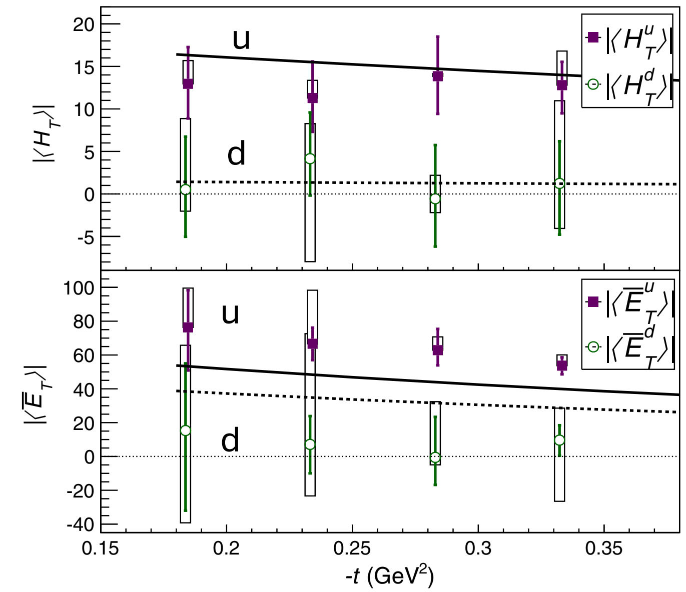

FIG. 6. Magnitude of the nucleon helicity-flip $\langle H_T \rangle$ (top) and nonflip $\langle \bar{E}_T \rangle$ (bottom) transversity terms for u (squares) and d (circles) quarks assuming no relative phase between them. The boxes around the points represent the variation of the results when their relative phase varies between 0 and π. Bars show the quadratic sum of the statistical and systematic uncertainties of the data. Solid (dashed) lines are calculations from the Goloskokov-Kroll model [14] for u (d) quark.

Deep Virtual η

- I.Bedlinsky *et al* [CLAS] Phys.Rev.C 95 (2017) 3, 035202
  - 6 GeV cross sections
  - Curves from GK ($d\sigma_T \gg d\sigma_L$)
    - $d\sigma_{TT} \gg d\sigma_{LT}$

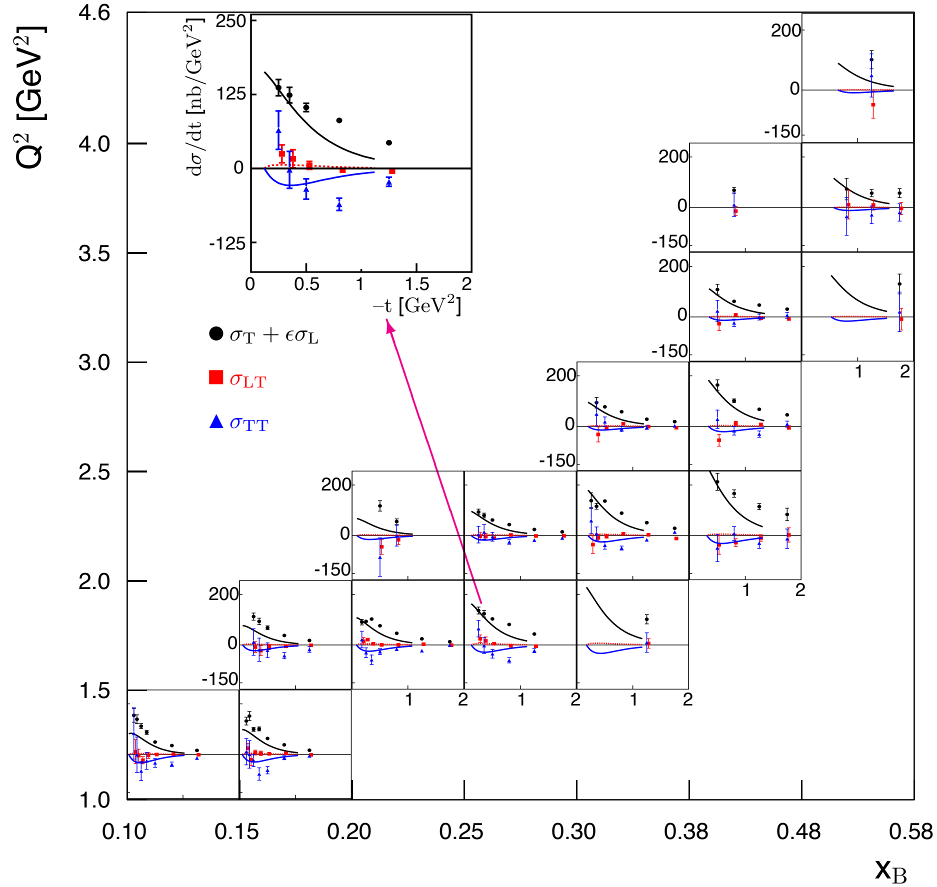

FIG. 13. The structure functions vs t for the different (Q^2,x_B) bins, extracted from the present experiment. Black circles: $d\sigma_U/dt$. Red squares: $d\sigma_{LT}/dt$. Blue triangles: $d\sigma_{TT}/dt$. The black, red, and blue curves are the corresponding results of the handbag-based calculation of Ref. [8]. The inset is an enlarged view of the bin with $x_B = 0.17$ and $Q^2 = 1.87$ GeV^2. The error bars are statistical only.

Comparison of Deep π^0 and η

- I.Bedlinsky *et al* [CLAS] Phys.Rev.C **95** (2017) 3, 035202
- Curves of Goloskokov & Kroll qualitatively accurate

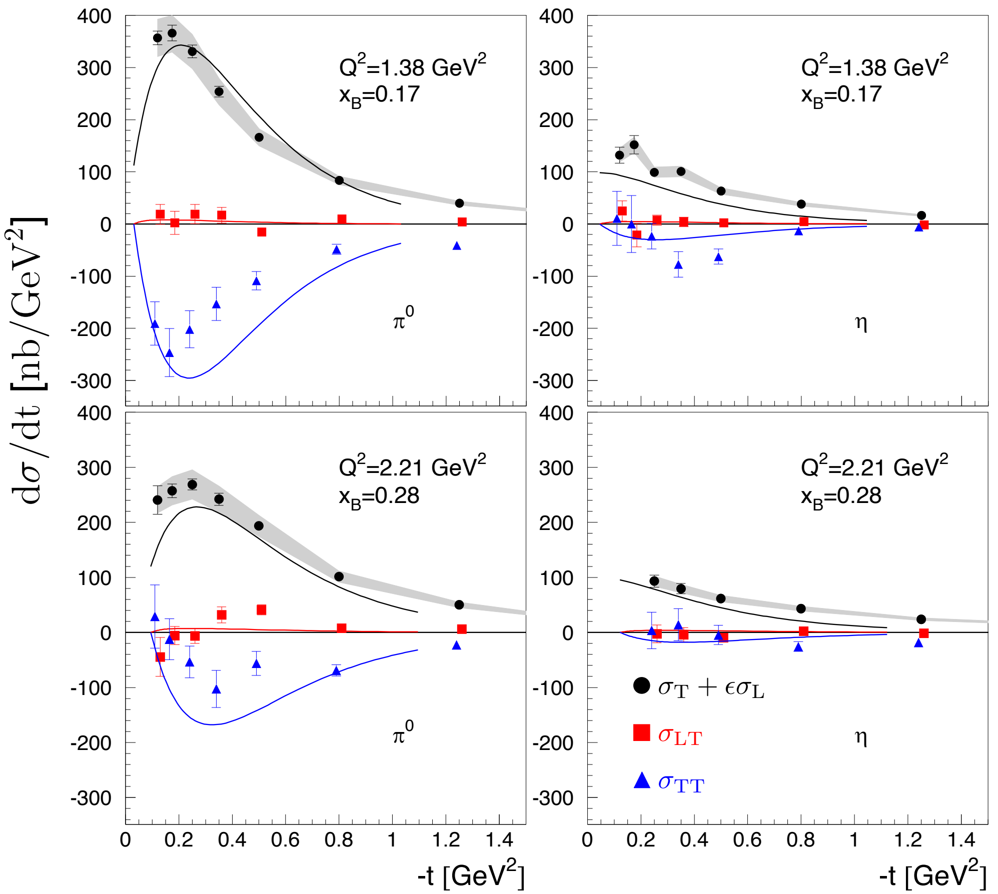

12 GeV: Hall A π^0

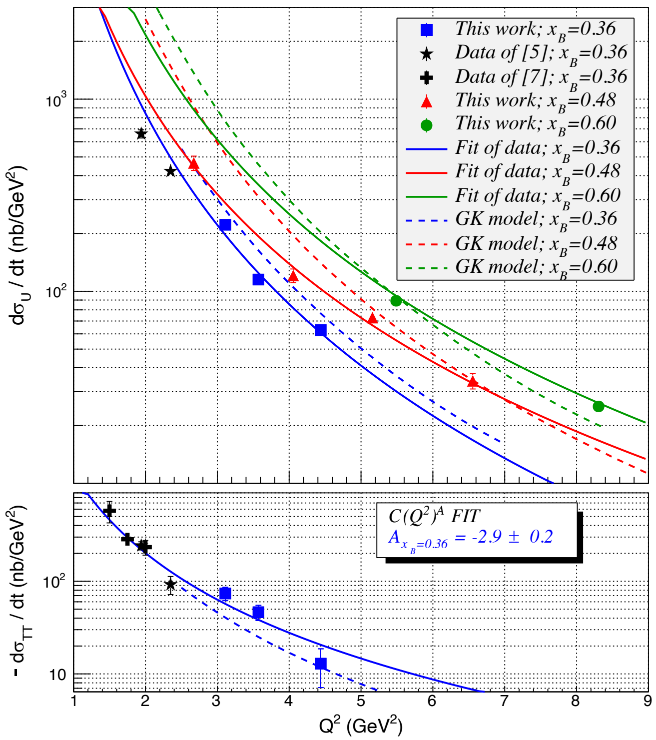

Hall C data in analysis

- Rosenbluth separations
- H, D targets

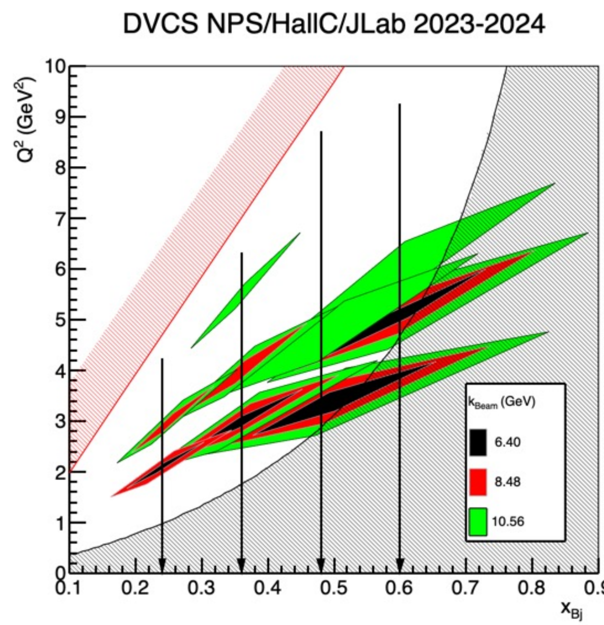

12 GeV: CLAS π^0 BSA

$$\frac{\sigma_{LT'}}{\sigma_0} \approx \frac{\sigma_{LT'}}{\sigma_T} \sim \frac{\mathcal{I}\mathrm{m}\left[\langle\overline{\mathcal{E}}_T\rangle\left\langle\widetilde{\mathcal{H}}\right\rangle + \langle\mathcal{H}_T\rangle\left\langle\widetilde{\mathcal{E}}\right\rangle\right]}{(1-\xi^2)\left|\langle\mathcal{H}_T\rangle\right|^2 + \frac{(t_0-t)}{8M^2}\left|\langle\overline{\mathcal{E}}_T\rangle\right|^2}$$

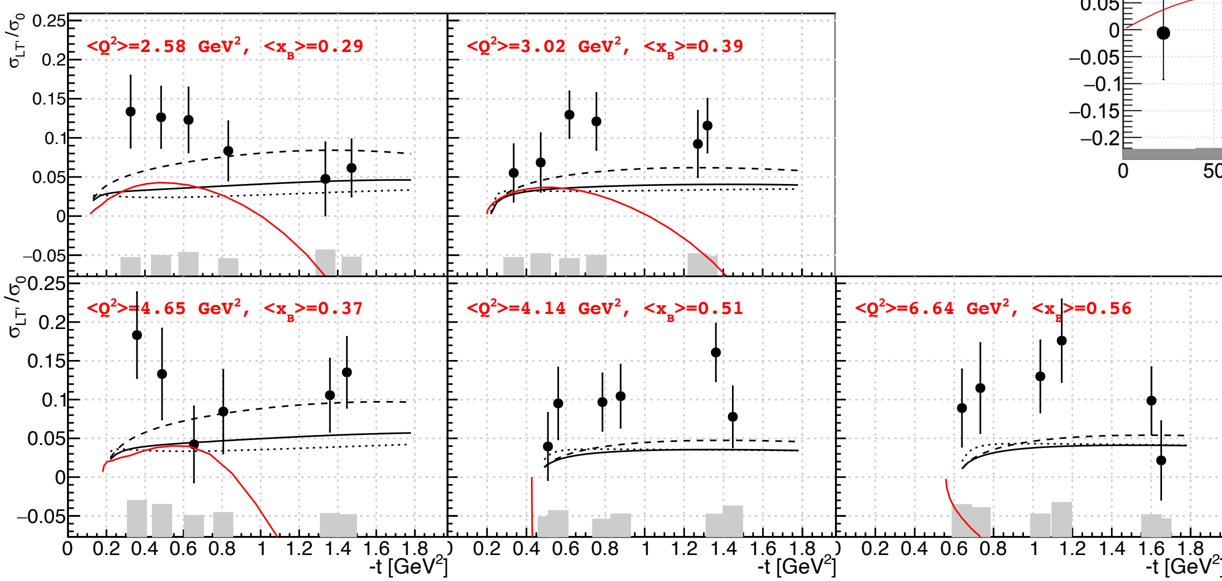

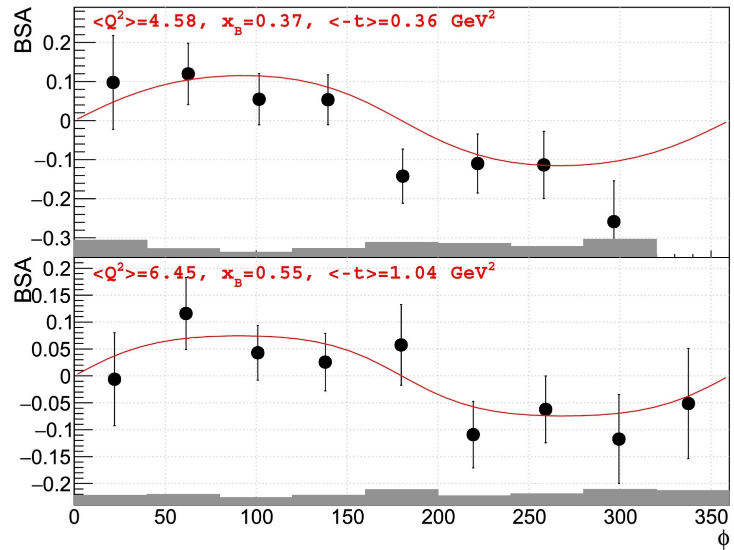

In progress:

- Full cross section
- Eta-production
- H, D targets...

Exclusive π^0 : COMPASS

M. Alexeev et al. [COMPASS],
*Phys.Lett.*B **805** (2020) 135454
arXiv:1093.12030

- $\langle Q^2 \rangle$ = 2.0 GeV²
- $\langle x_B \rangle = 0.093$

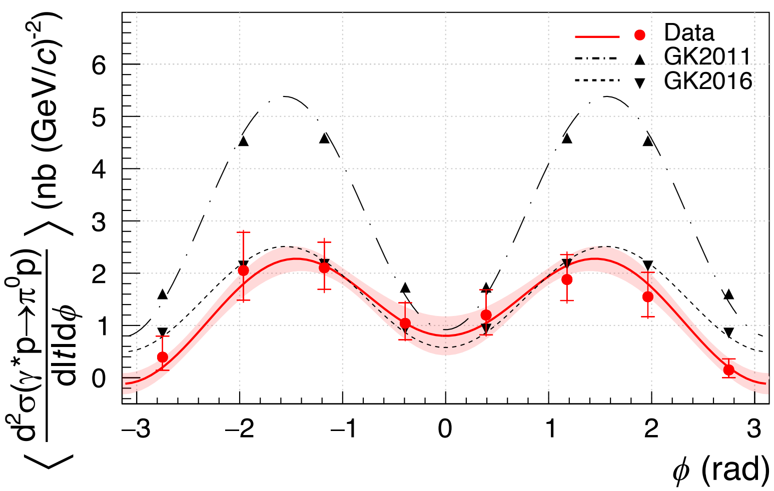

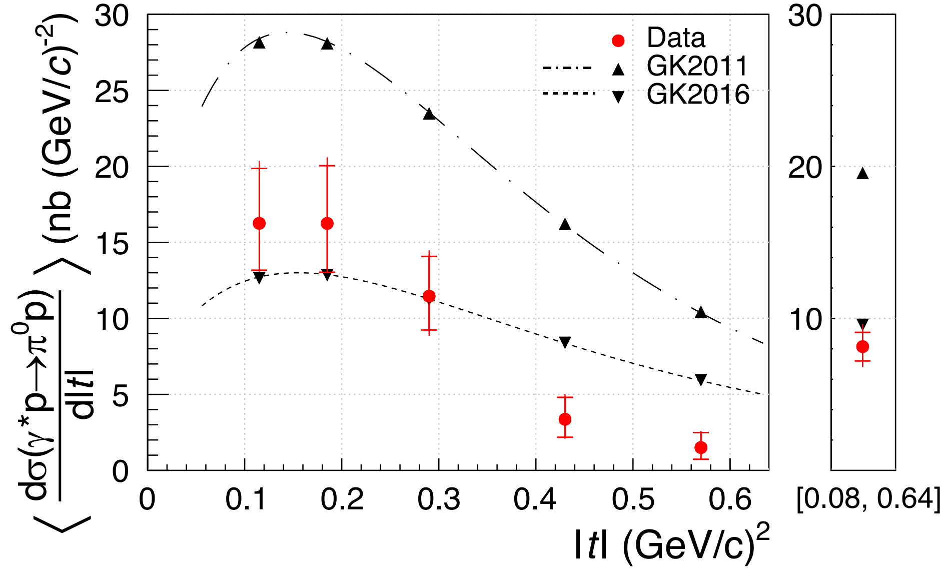

DVCS: What do we measure?

- Cross sections and asymmetries
  - Linked to CFFs, not GPDs
  - Very complicated structure of cross section
  - Need polarization observables to extract CFFs
- Azimuthal distribution analyzes polarization of virtual photon
- Longitudinal and transverse polarized targets
  - Longitudinal is hard
  - Transverse is extremely hard (except at EIC!)
    - Only existing data are from HERMES

DVCS Analysis Techniques

- Monte Carlo simulation of the full DVCS amplitude → cross section and/or Asymmetries. Adjust model to fit data.
  - Mostly used only when allows restriction to just one GPD
    - H_{glue} for HERA
    - Isoscalar H for coherent ^{4}He
- Simplistic Fourier analysis (recommended by Kumericki & Mueller)
  - Works well in domains where BH is weak
- Fit semi-empirical forms
  - BSA = $\alpha \sin\phi/[1 + \beta \cos\phi]$
- Monte Carlo simulation of the structure of DVCS observables (perhaps neglecting a few "kinematically suppressed" terms

Also need to include "radiative effects"

"BMK"

- A.Belitsky, D.Mueller, PhysRev D **82**, 074010 (2010)
- Kinematic factors
- Bilinear CFF terms
- Linear CFF terms times elastic FF

$$d\sigma = \frac{\alpha^3 x_B y^2}{8\,\pi\,\mathcal{Q}^4\sqrt{1+\epsilon^2}}\left|\frac{\mathcal{T}}{e^3}\right|^2 dx_B d\mathcal{Q}^2 d|t| d\phi\,.$$

$$\epsilon^2 \equiv 4x_B^2\frac{M^2}{\mathcal{Q}^2}\,,$$

$$\mathcal{T}^2 = |\mathcal{T}^{\rm BH}|^2 + |\mathcal{T}^{\rm DVCS}|^2 + \mathcal{I}$$

$$|\mathcal{T}^{\rm DVCS}|^2 = \frac{e^6}{y^2\mathcal{Q}^2}\left\{c_0^{\rm DVCS} + \sum_{n=1}^{2}\left[c_n^{\rm DVCS}\cos(n\phi) + s_n^{\rm DVCS}\sin(n\phi)\right]\right\}$$

$$c_{0,\rm unp}^{\rm DVCS} = 2\frac{2-2y+y^2+\frac{\epsilon^2}{2}y^2}{1+\epsilon^2}\,\mathcal{C}_{\rm unp}^{\rm DVCS}(\mathcal{F},\mathcal{F}^*) + \dots$$

$$\left\{\begin{matrix} c_{1,\rm unp}^{\rm DVCS} \\ s_{1,\rm unp}^{\rm DVCS}\end{matrix}\right\} = \frac{8K}{(2-x_B)(1+\epsilon^2)}\left\{\begin{matrix} (2-y) \\ -\lambda y\sqrt{1+\epsilon^2}\end{matrix}\right\}\left\{\begin{matrix} \Re{\rm e} \\ \Im{\rm m}\end{matrix}\right\}\mathcal{C}_{\rm unp}^{\rm DVCS}(\mathcal{F}_{\rm eff},\mathcal{F}^*)$$

$$\mathcal{I} = \frac{\pm e^6}{x_B y^3 t \mathcal{P}_1(\phi)\mathcal{P}_2(\phi)}\left\{c_0^{\mathcal{I}} + \sum_{n=1}^{3}\left[c_n^{\mathcal{I}}\cos(n\phi) + s_n^{\mathcal{I}}\sin(n\phi)\right]\right\},$$

$$c_n^{\mathcal{I}} = C_{++}(n)\,\Re{\rm e}\,\mathcal{C}_{++}^{\mathcal{I}}(n|\mathcal{F}) + C_{0+}(n)\,\Re{\rm e}\,\mathcal{C}_{0+}^{\mathcal{I}}(n|\mathcal{F}_{\rm eff}) + C_{-+}(n)\,\Re{\rm e}\,\mathcal{C}_{-+}^{\mathcal{I}}(n|\mathcal{F}_T)\,,$$

$$s_n^{\mathcal{I}} = S_{++}(n)\,\Im{\rm m}\,\mathcal{S}_{++}^{\mathcal{I}}(n|\mathcal{F}) + S_{0+}(n)\,\Im{\rm m}\,\mathcal{S}_{0+}^{\mathcal{I}}(n|\mathcal{F}_{\rm eff}) + S_{-+}(n)\,\Im{\rm m}\,\mathcal{S}_{-+}^{\mathcal{I}}(n|\mathcal{F}_T)\,.$$

Real & Imaginary part of [DVCS*BH] Interference

- A careful examination of the kinematic pre-factors of the $|BH|^2$, Re[DVCS*BH] and $|DVCS|^2$ show they contain different powers of s=(k+P)^2.
- Im[DVCS*BH] interference from spin-dependent cross sections $d\sigma(+) - d\sigma(-)$, since BH is real
- Two methods for separation of the Re[DVCS*BH] from |DVCS|^2
  - Beam charge difference HERMES, HERA, COMPASS
  - Beam energy-dependence "Generalized Rosenbluth Separation":
    - M.Defurne, *et al* [Hall A], Nature Commun. **8** (2017) 1, 1408
    - 2023-2024 Hall C "Neutral Particle Spectrometer (NPS)" data

A first test of factorization at large x_B

- C.Muñoz Camacho, *et al.* [Hall A], *PRL* **97**:262002

- Some ambiguities in how to extract Re[DVCS*BH]+|BH|^2

- Q^2-independence of the imaginary part of the interference
  - Dominance of Twist-2 (GPD)
  - « VGG » model correct to 30%

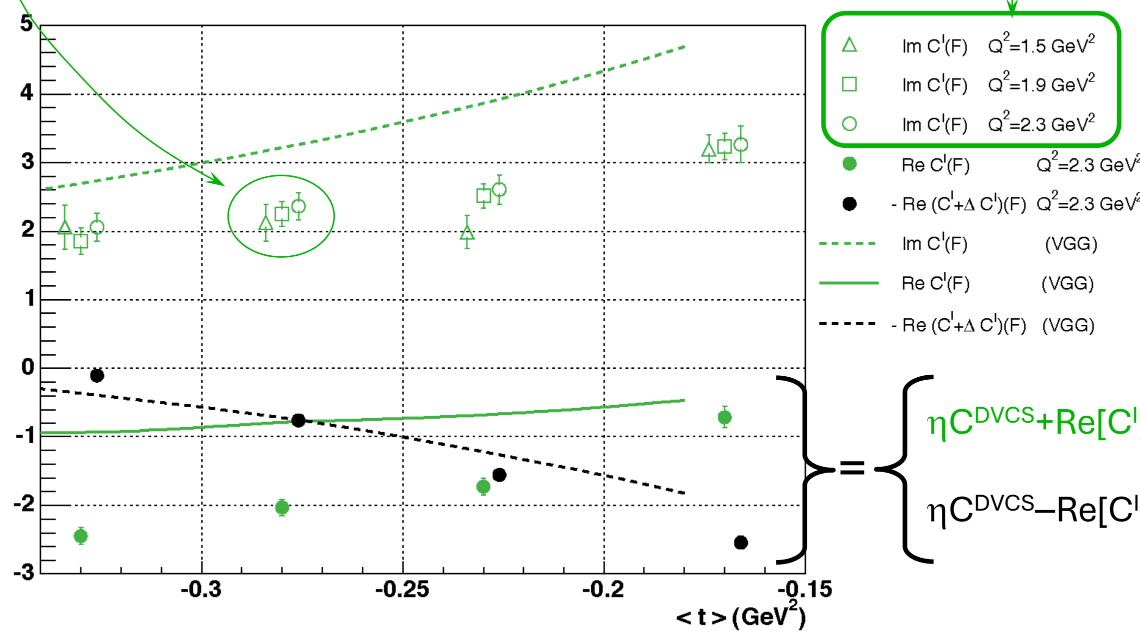

$$= \begin{cases} \eta C^{DVCS} + \mathrm{Re}[C^I] \\ \eta C^{DVCS} - \mathrm{Re}[C^I + \Delta C^I] \end{cases}$$

Separation of Re[DVCS*BH] and |DVCS|^2

- M.Defurne, *et al* [Hall A], Nature Commun. **8** (2017) 1, 1408
- 2 beam energies, 3 Q^2 values at x=0.36. “6 GeV”
- Analyzed dσ results in BMP helicity frame (q,q’)
- Data preferred inclusion of either Gluon transversity: helicity flip GPD (HT) or NLO $(q\bar{q}g)$ amplitude

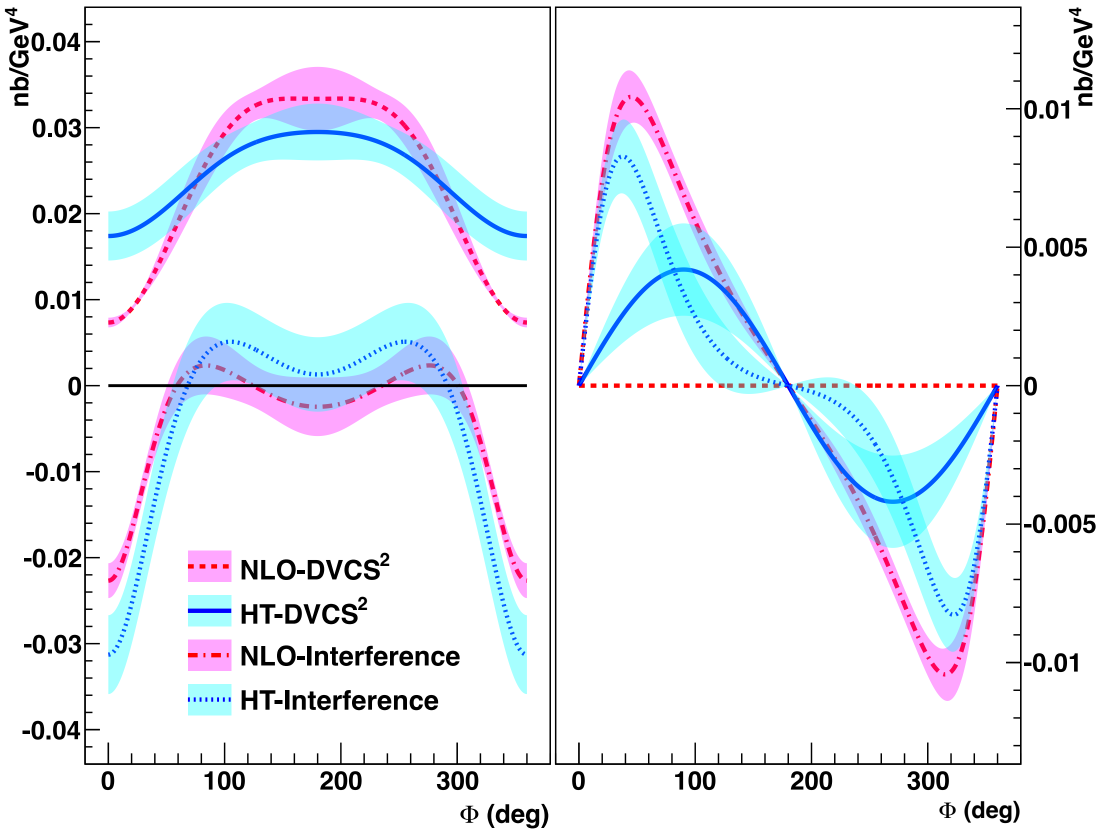

Hall A 12 GeV DVCS

PHYSICAL REVIEW LETTERS **128,** 252002 (2022)

TABLE I. Main kinematic variables for each of the nine (Q^2, x_B) settings where the DVCS cross section is reported. E_b is the incident electron energy, E_γ and $-t_{\min}$ correspond to a final state photon emitted parallel to $\mathbf{q} = \mathbf{k} - \mathbf{k}'$ at the nominal Q^2, x_B values listed. For each setting, the cross section is measured as a function of t (3 to 5 bins depending on the setting) and in 24 bins in ϕ. The accumulated charge, corrected by the acquisition dead time, is listed in the row labeled $\int Qdt$. The last row of the table indicates the number of statistically independent measurements (bins) for each x_B setting, including helicity dependence.

Setting	Kin-36-1	Kin-36-2	Kin-36-3	Kin-48-1	Kin-48-2	Kin-48-3	Kin-48-4	Kin-60-1	Kin-60-3
x_B		0.36			0.48			0.60	
E_b (GeV)	7.38	8.52	10.59	4.49	8.85	8.85	10.99	8.52	10.59
Q^2 (GeV^2)	3.20	3.60	4.47	2.70	4.37	5.33	6.90	5.54	8.40
E_γ (GeV)	4.7	5.2	6.5	2.8	4.7	5.7	7.5	4.6	7.1
$-t_{\min}$ (GeV^2)	0.16	0.17	0.17	0.32	0.34	0.35	0.36	0.66	0.70
$\int Qdt$ (C)	1.2	1.7	1.3	2.2	2.2	3.7	5.7	6.4	18.5
Number of data bins		672			912			480	

- Analyzed full energy, Q^2, ϕ, beam helicity dependence
- Helicity conserving terms *e.g.* $\mathcal{H}_{++}$ shown, error bands include effects of $\mathcal{H}_{0+}$ and $\mathcal{H}_{-+}$

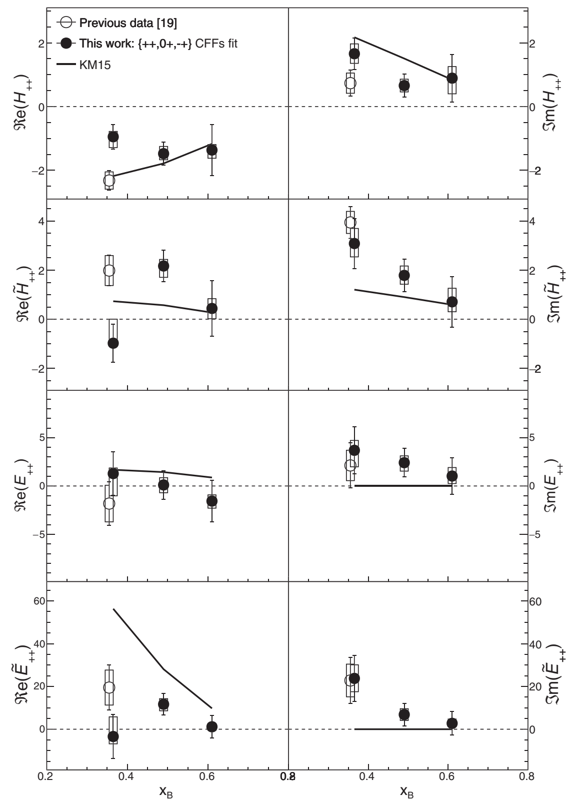

FIG. 4. Values of the helicity-conserving CFFs, averaged over t, as a function of x_B. Bars around the points indicate statistical uncertainty and boxes show the total systematic uncertainty. The fit results of previous data [19] at $x_B = 0.36$ are displayed with the open markers. The average t values are -0.281 GeV^2 [19] and -0.345, -0.702, -1.050 GeV^2 at $x_B = 0.36$, 0.48, 0.60, respectively. The solid lines show the KM15 model [29].

CLAS proton DVCS

- H.Jo *et al. (CLAS Collaboration), Phys. Rev. Lett.***115***, 212003 (2015).*
- Extraction of Re,Im[H] (also fitting $\widetilde{H}$)

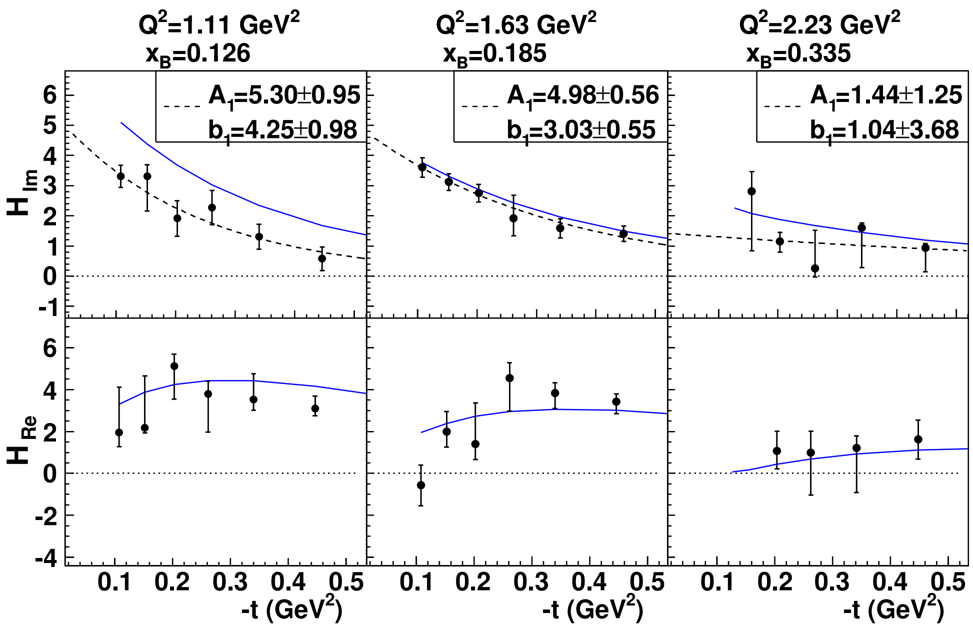

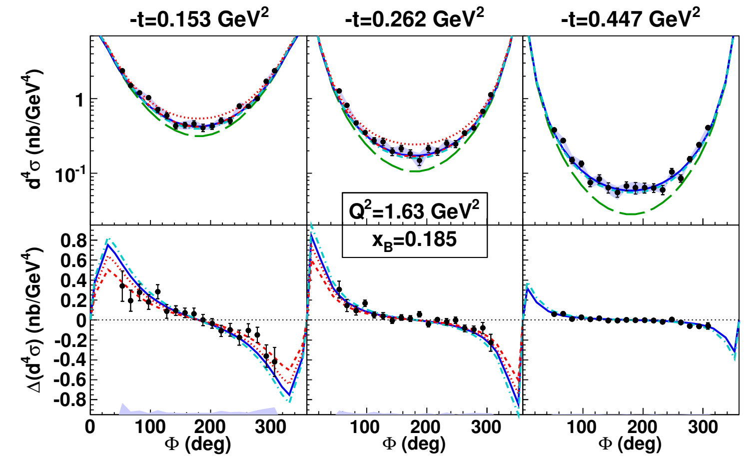

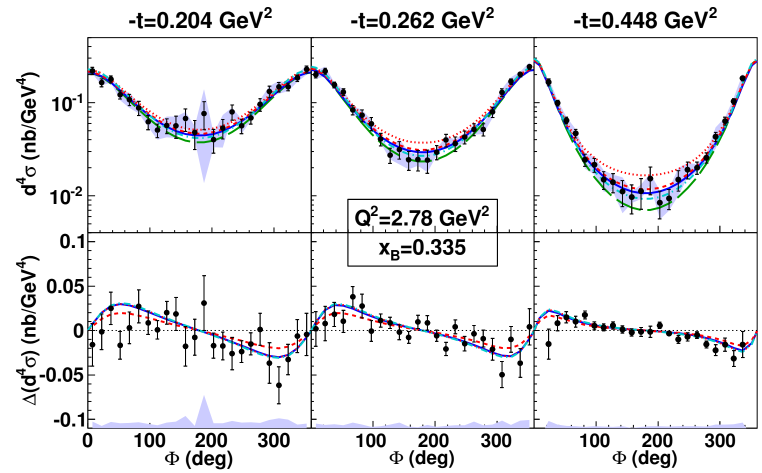

CLAS Longitudinally polarized NH_3 target

- E.Seder *et al. [CLAS]* Phys.Rev.Lett. 114 (2015) 3, 032001
- Extensive measurements, primary sensitivity to $\mathrm{Im}\left[\tilde{\mathcal{H}}\right]$

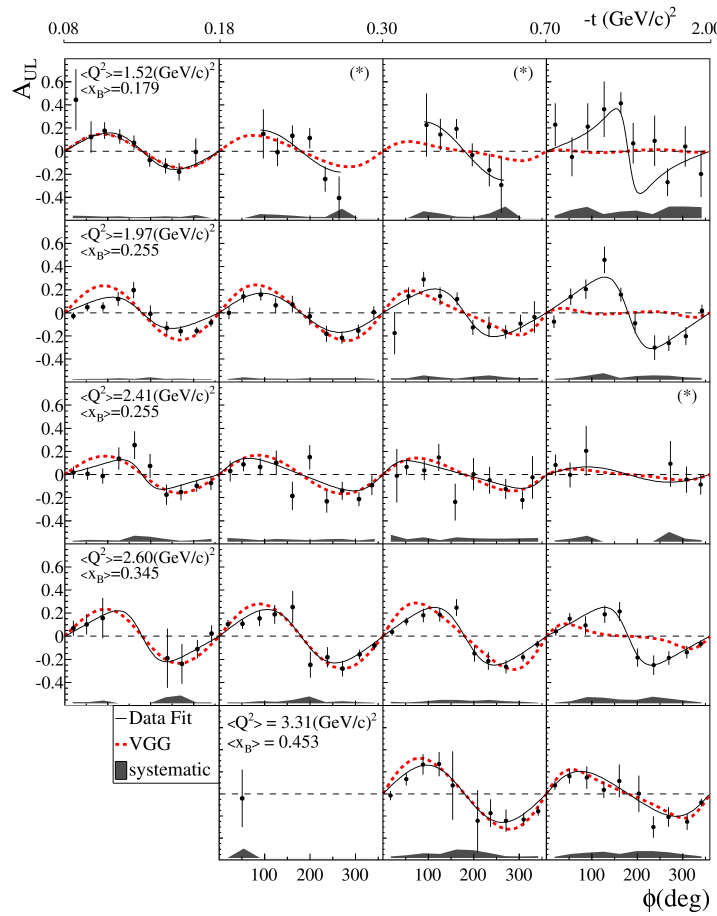

CLAS Longitudinally polarized target

- E.Seder *et al. [CLAS]* Phys.Rev.Lett. 114 (2015) 3, 032001
- Amplitude of sinϕ term of target single-spin asymmetry

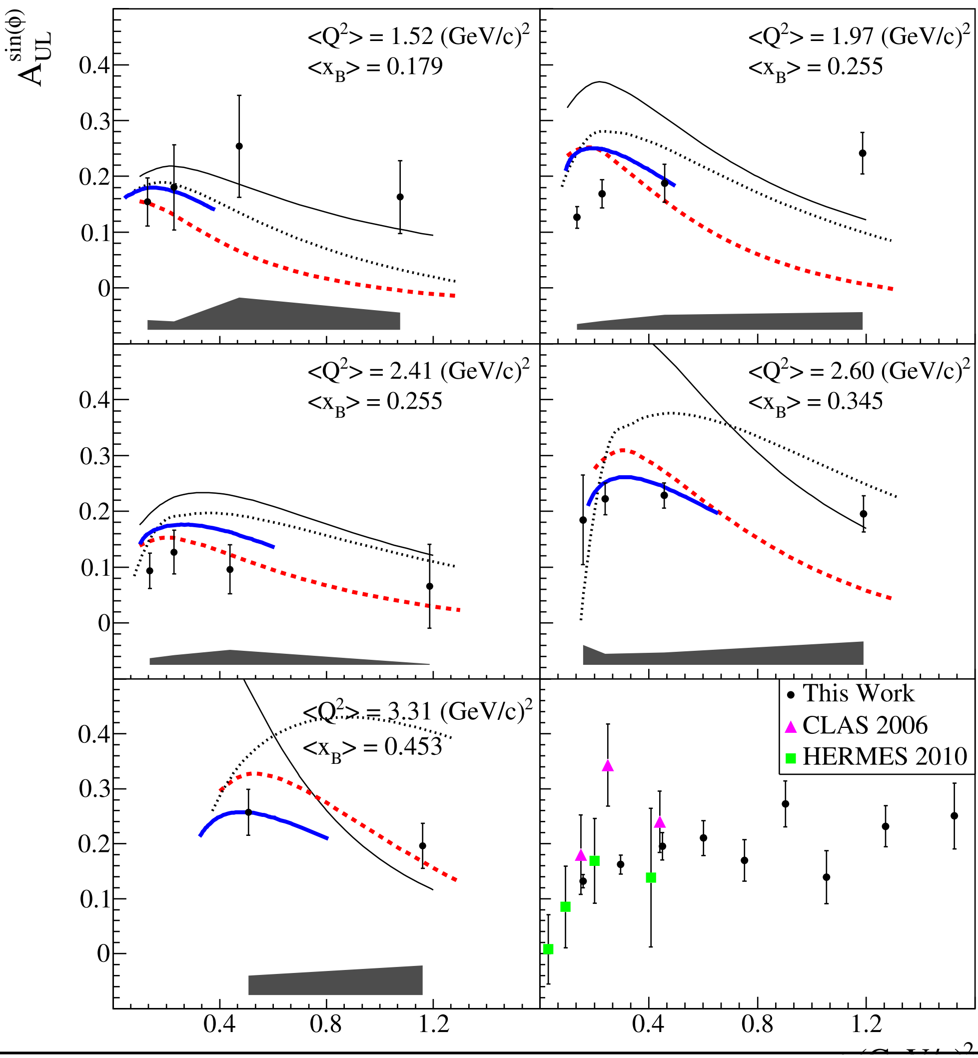

FIG. 4. (Color online) First five plots: $-t$ dependence of the $\sin\phi$ amplitude of A_{UL} for each Q^2-x_B bin. The shaded bands represent the systematic uncertainties. The curves show the predictions of four GPD models: i) VGG [18] (red-dashed), ii) GK [20] (black-dotted), KMM12 [21] (blue-thick solid), GGL [22] (black-solid). Bottom right plot: comparison of the $\sin\phi$ amplitude of A_{UL} as a function of $-t$ for the results of this work (black dots) integrated over all Q^2 and x_B values ($\langle Q^2\rangle$ = 2.4 (GeV/c)^2, $\langle x_B\rangle$ = 0.31), the HERMES results [13] (green squares) at $\langle Q^2\rangle$ = 2.459 (GeV/c)^2, $\langle x_B\rangle$ = 0.096, and the previously published CLAS results [12] (pink triangles), at $\langle Q^2\rangle$ = 1.82 (GeV/c)^2, $\langle x_B\rangle$ = 0.28.

First CLAS12 proton DVCS results

- G.Christiaens *et al.* [CLAS], Phys. Rev. Lett. **130** (2023) 211902

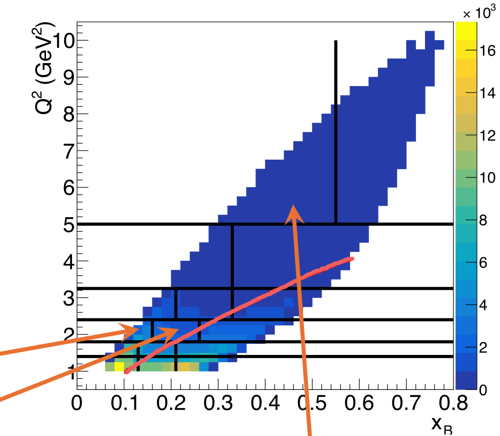

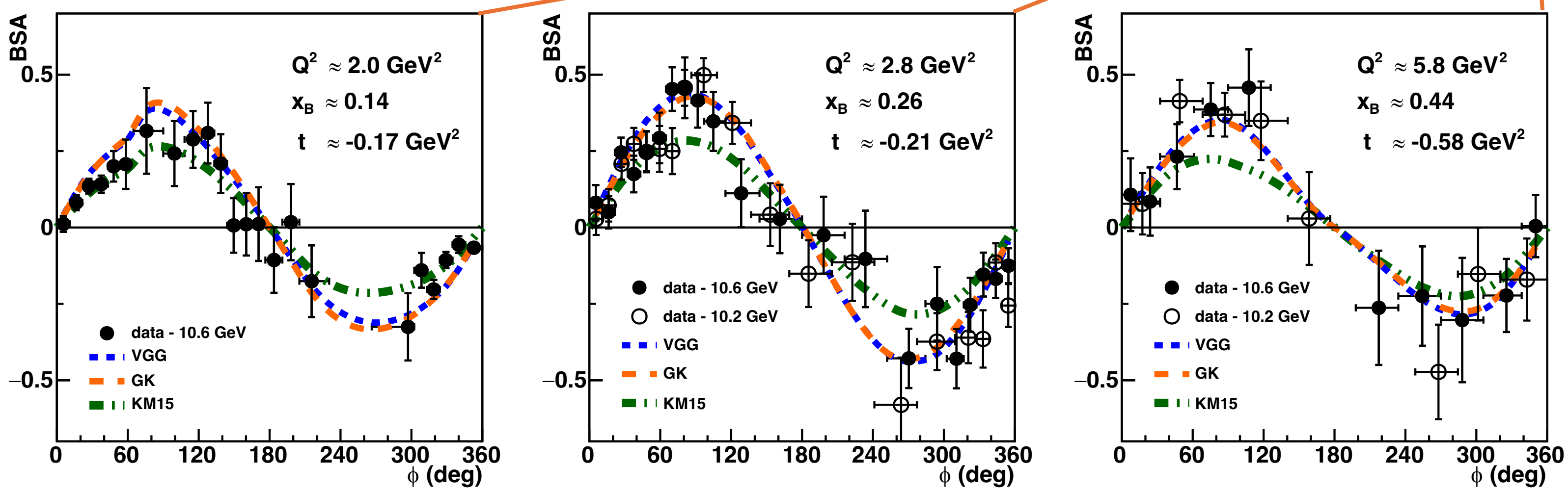

HERMES DIS2012

Exclusive Measurement

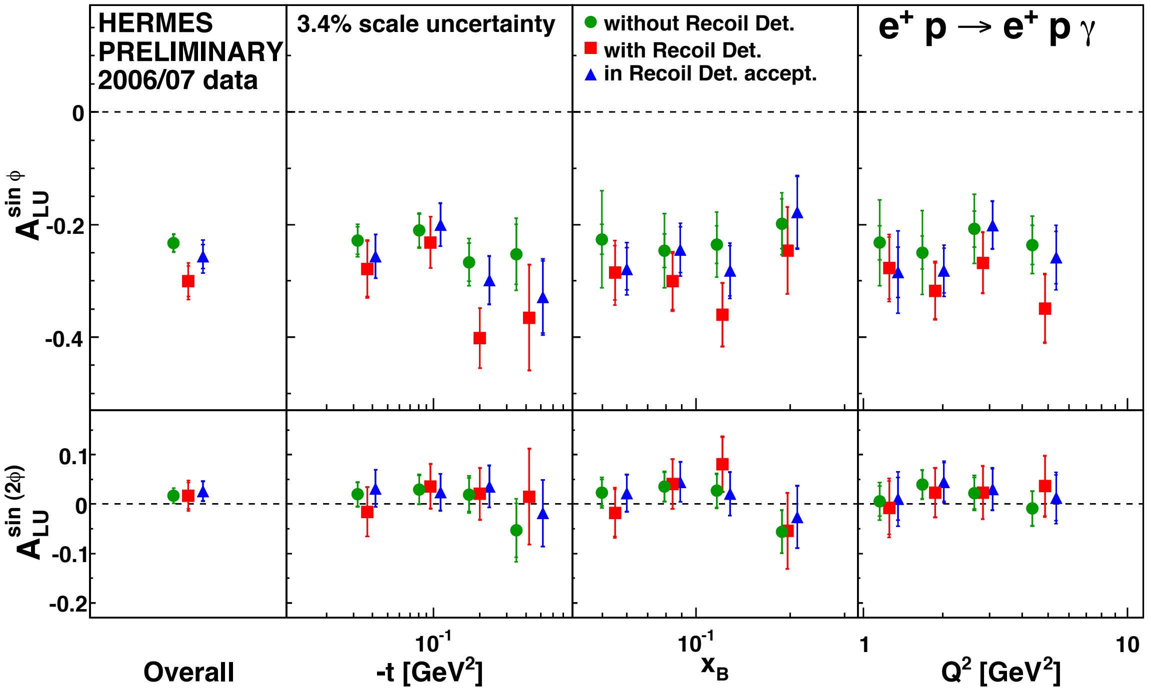

15

Beam-Charge Asymmetries

A. Airapetian et al, JHEP (2012), submitted http://arxiv.org/abs/1203.6287

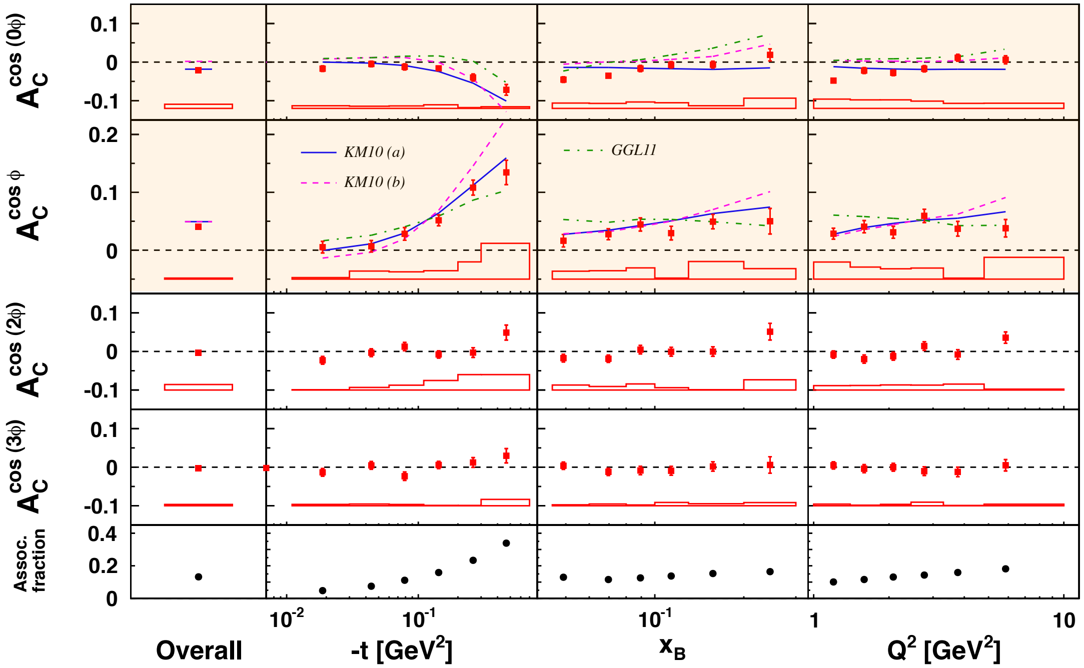

Kumerički and Müller, Nucl. Phys. **B841** (2010) http://arxiv.org/abs/0904.0458

G. Goldstein, J. Hernandez and S. Liuti, **Phys. Rev. D84** (2011) http://arxiv.org/abs/1012.3776

Beam Charge Asymmetries access Re($\mathcal{H}$)

11

Beam-Spin Asymmetries

A. Airapetian et al, JHEP (2012), submitted http://arxiv.org/abs/1203.6287

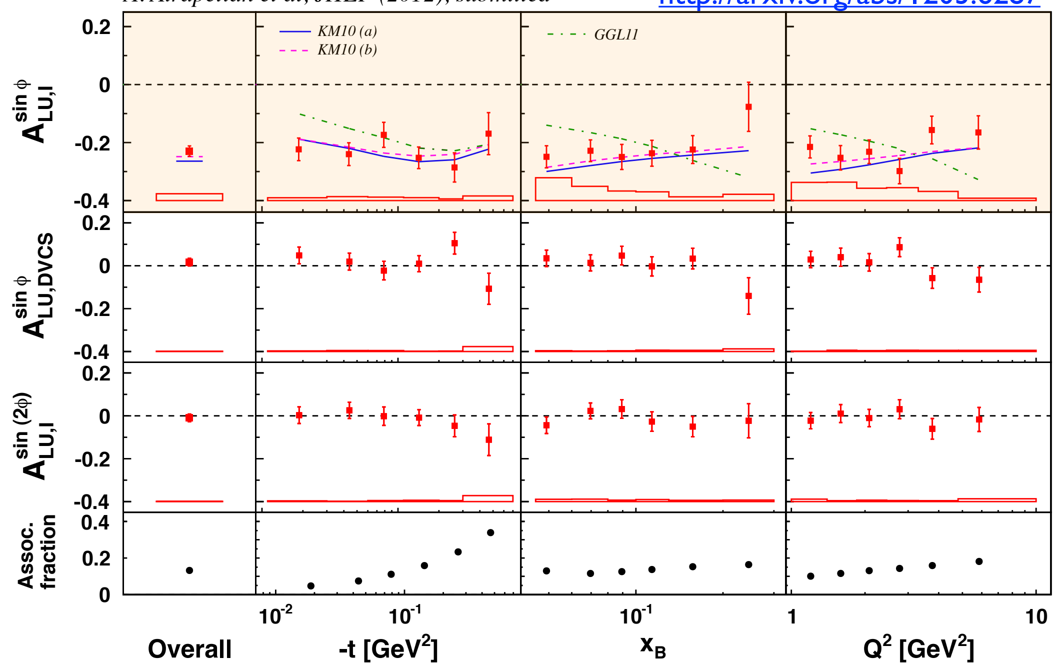

Beam Helicity Asymmetries access Im($\mathcal{H}$)

12

Neutron DVCS: An old, provocative Plot

- M.Mazouz Phys.Rev.Lett. **99** (2007) 242501
- Fit model of E GPD to one (ξ,Q^2) data point.
- Integrate the model over x.
- HERMES data was transversely polarized *p*

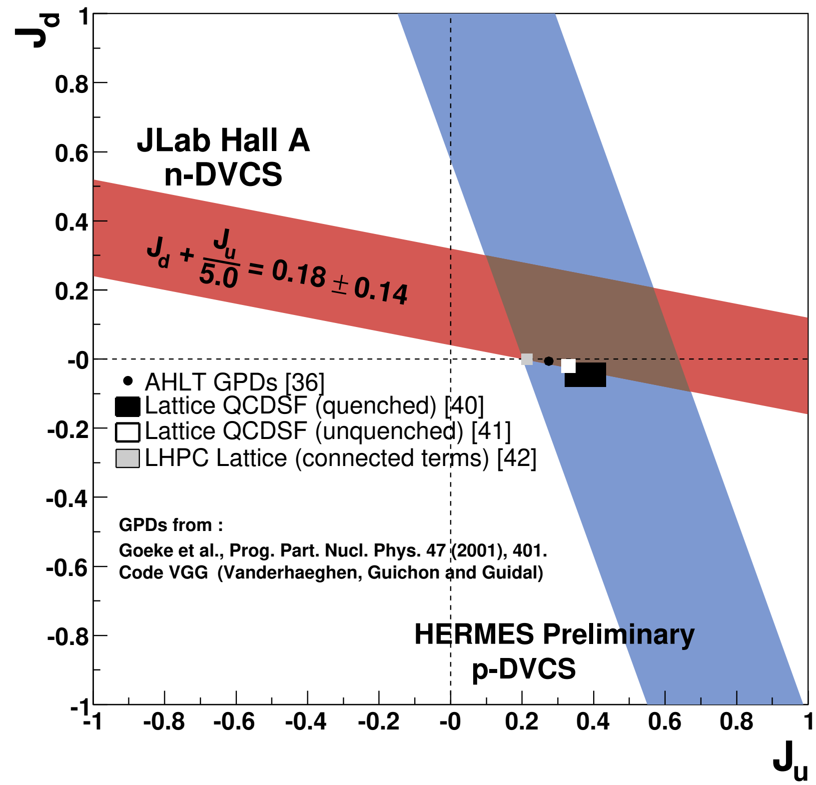

Neutron DVCS

- M.Benali, et al. [Hall A], Nature Phys. **16** (2020) 2, 191
- Combined D,H analysis $x_B = 0.36$

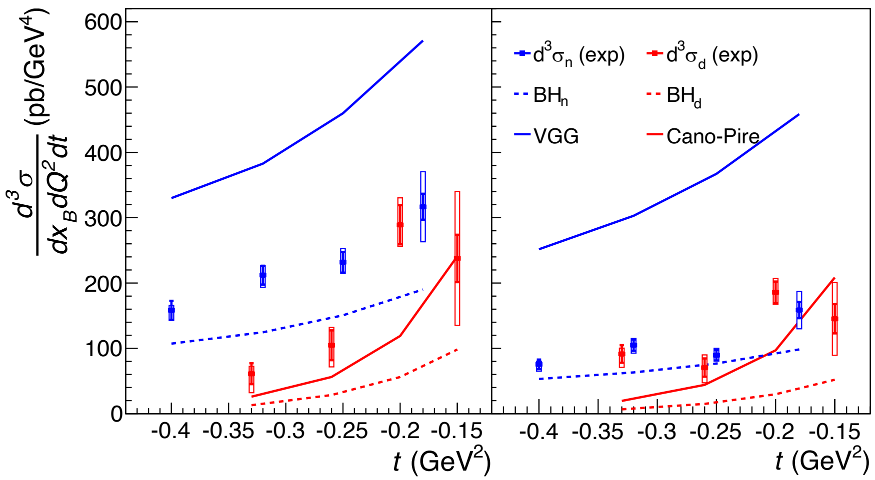

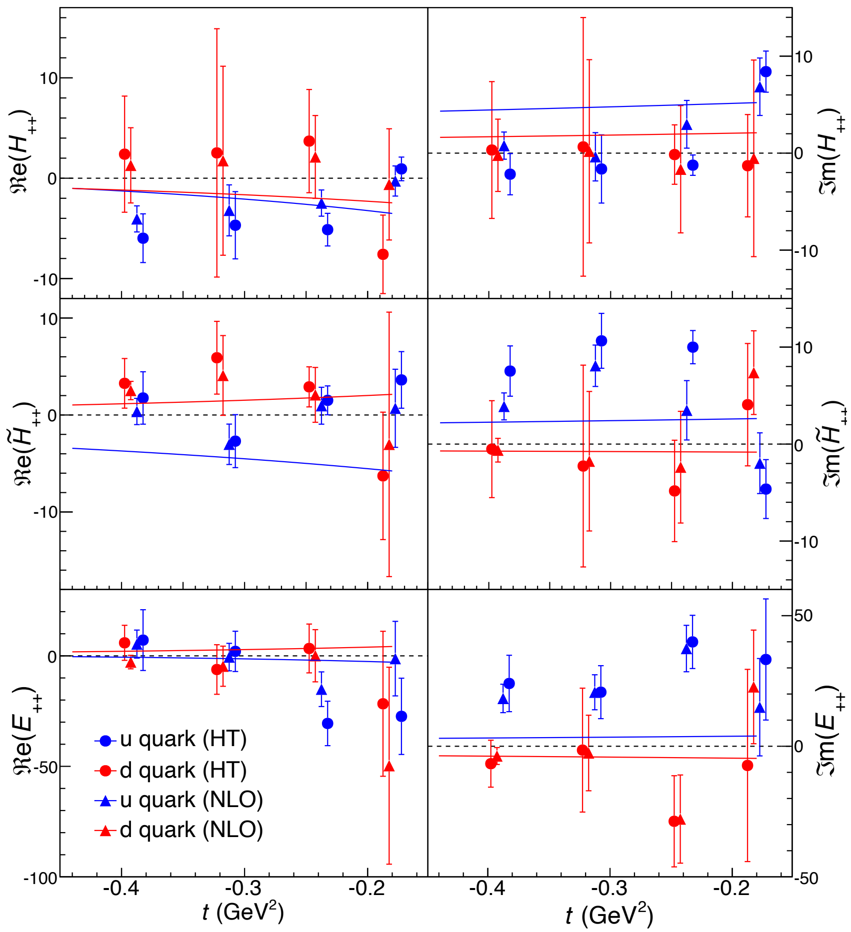

DVCS at HERA

- Next three slides are from review by G. Wolf arXiv 0907.1217
- This slide, GPD model of Freund

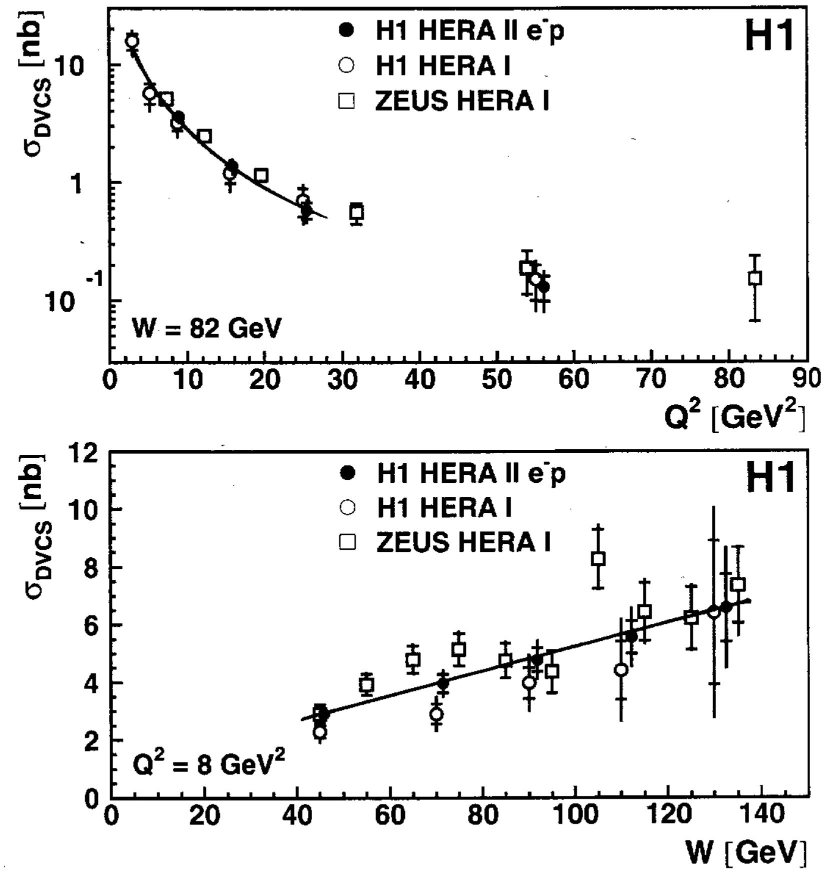

DVCS at HERA

- *t*-dependence

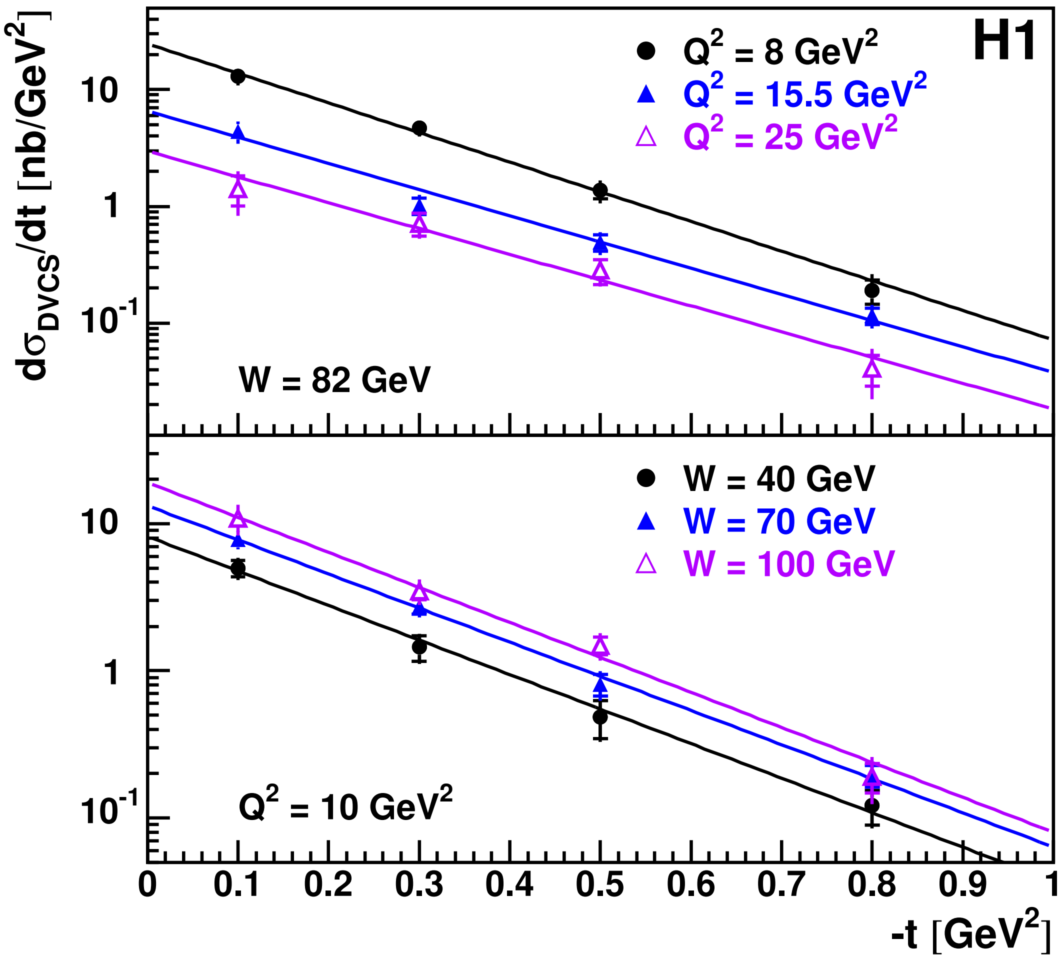

DVCS at HERA

- The DVCS cross section as a function of the scaling variable $\tau = \frac{Q^2}{Q_S^2(x)}$, for W = 82 GeV and Q^2 = 8, 15.5, 25 GeV^2 (top), and for W = 40,80,100 GeV, Q^2 = 10 GeV^2 (bottom), as measured by H1.
- The dashed curve shows the prediction of the dipole model

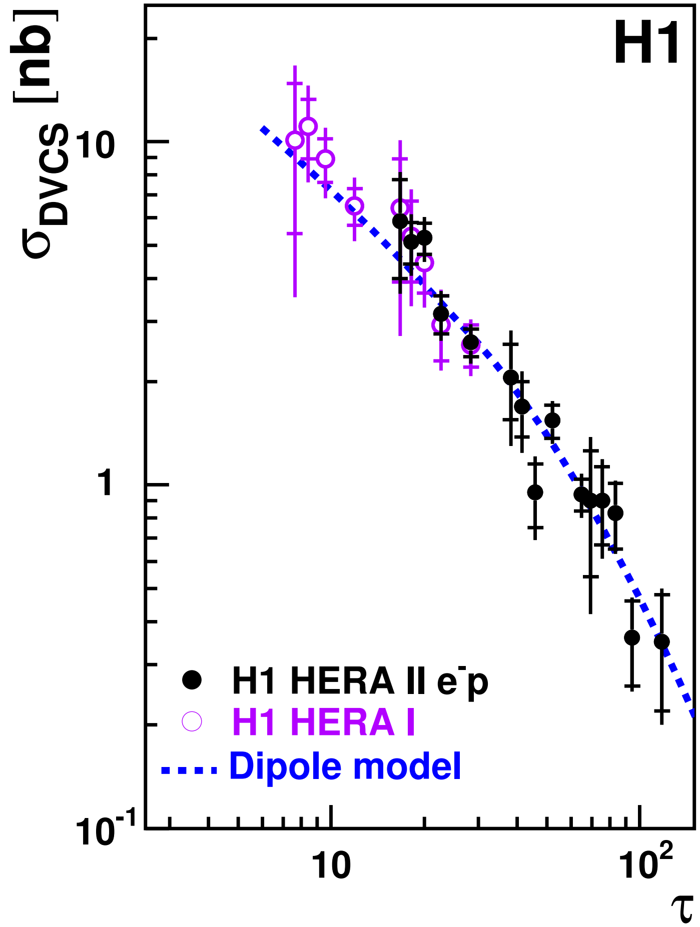

Gluon Radius of Proton? DVCS

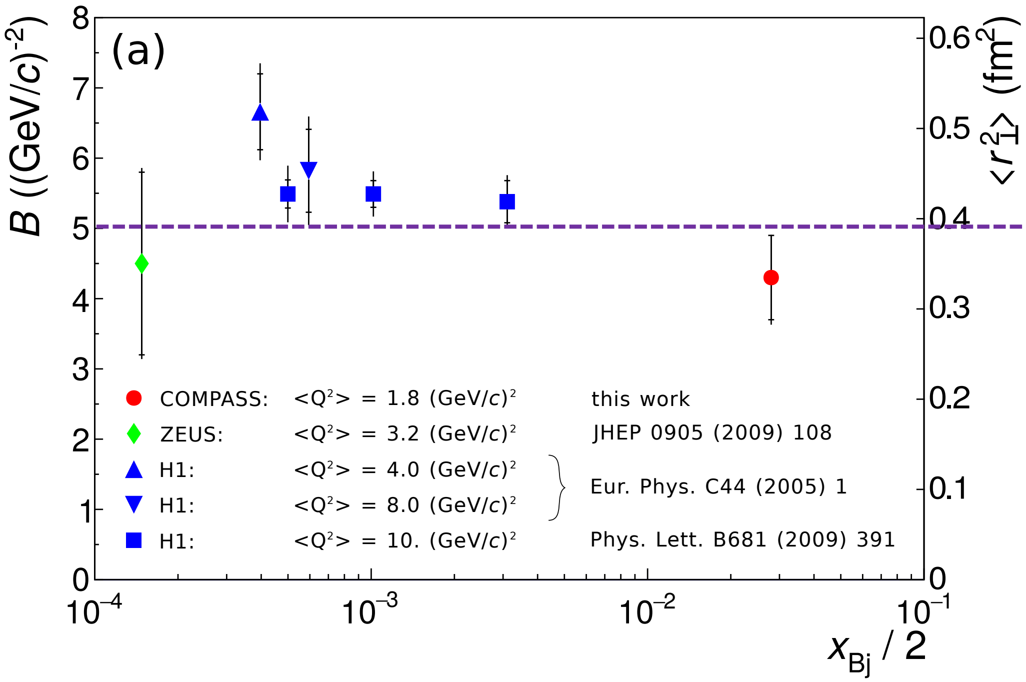

Phys.Lett.B **793** (2019) 188-194
arXiv:1802.02739

- COMPASS, HERA *t*-slope of *H(x/2,x/2,t)* at small-*x*
- Smaller than charge radius
  - 0.84 fm
- Evidence for low-*x* growth ~log(1/x)?
  - Gribov diffusion

$$\sqrt{\langle r_\perp^2 \rangle} = \hbar c \sqrt{2B} \approx 0.62 \text{ fm}$$

~50% of gluon momentum sum-rule is at x>0.1
How are these gluons distributed radially?

Model Fits: DVCS

R. Akhunzyanov *et al.* [COMPASS], Phys.Lett.B **793** (2019) 188-194 arXiv:1802.02739

- COMPASS, HERA *t*-slope of H(x/2,x/2,t) at small-x
- Kumericki Mueller (KM)
- Goloskokov Kroll
- What do these models do at high-*x*?

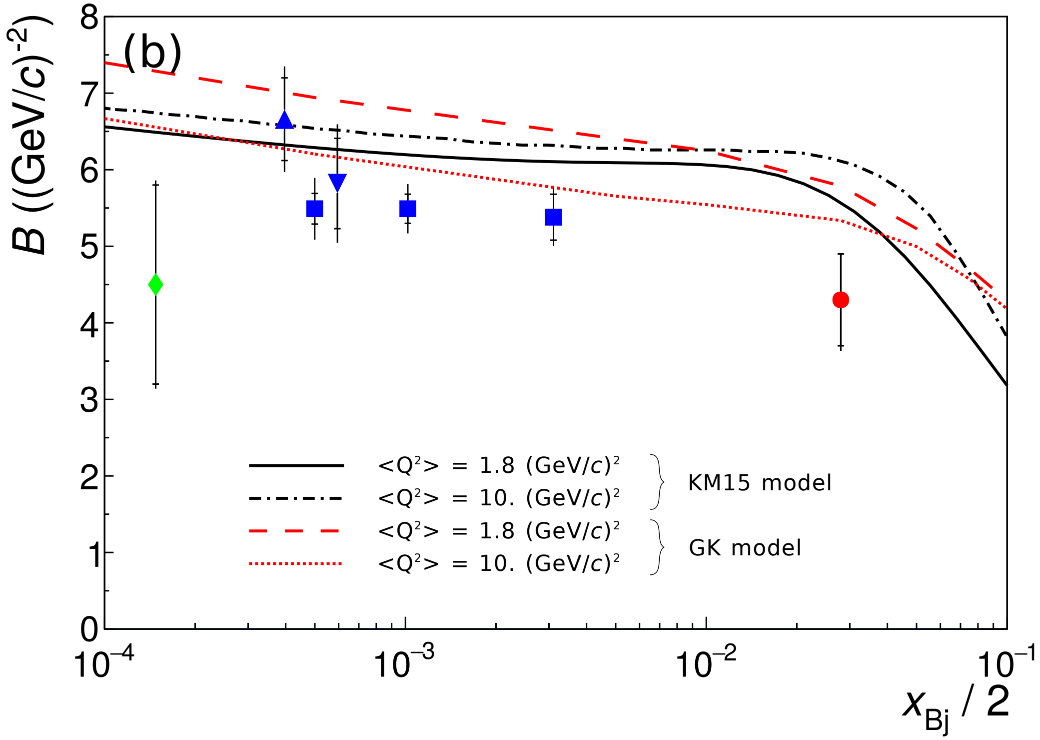

Conclusions

- There is now a large data base of 1000s of DVCS measurements
  - Cross sections
  - Single and double spin asymmetries
- Local and Global Fits enable separations of Compton Form Factors (CFFs), including flavor separations.
- Global fits can also test assumptions of factorization, NLO contributions and Higher Twist (both kinematic & dynamic)
- A great deal of Jlab 12 GeV data is on tape, in various stages of analysis and publication, and more data planned.

Epilogue

Radiative Corrections

Radiative Corrections to BH & DVCS

- M. Vanderhaeghen, et al., Phys Rev C **62,** 025501 (2000)
- I.Akushevich and A. Ilyich, Phys Rev D **85**, 053008 (2012)
- A. Afanasev, I. Akushevich, et al, Phys Rev D **66** (2002) (EXCLURAD)

- Figures that follow are from M.V. PRC **62**

Virtual Radiative Corrections

Vertex, Self-Energy, Vacuum-Polarization corrections to BH

Vertex, Vacuum-Polarization corrections to VCS

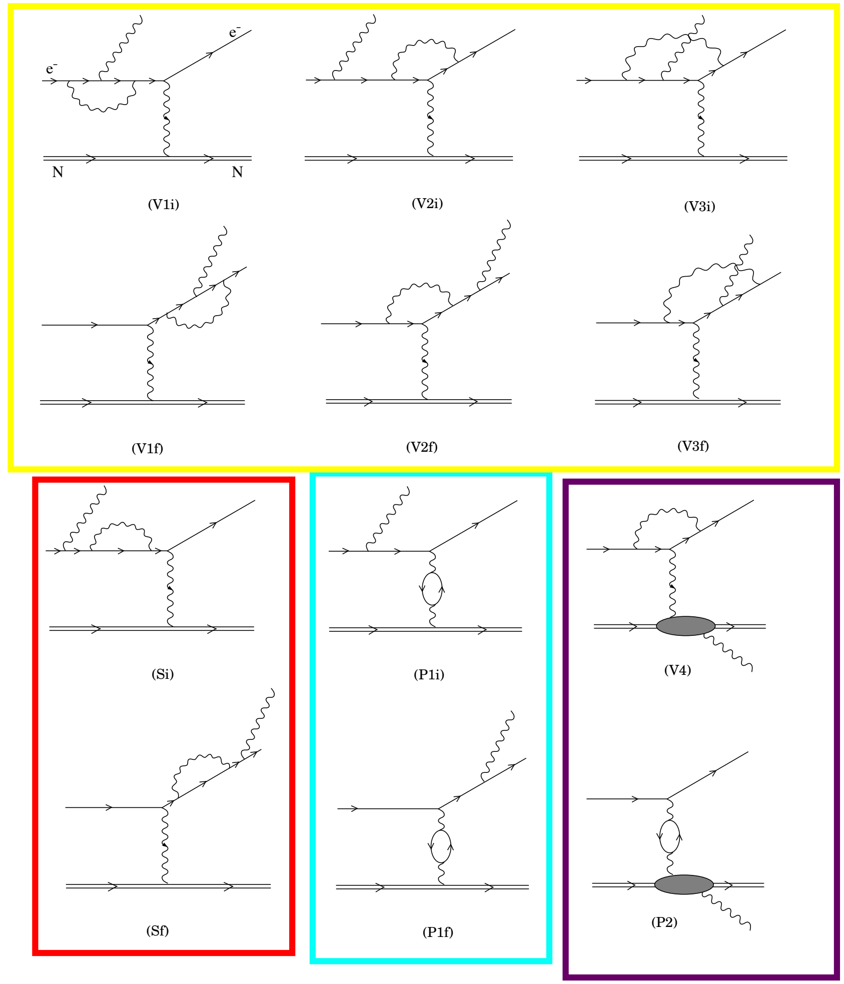

FIG. 2. First order virtual photon radiative corrections to the $ep \to ep\gamma$ reaction.

41

Virtual Radiative Corrections

Intrinsically different for BH & VCS

Vacuum-Polarization
BH: $1/[1+\Pi(t)]$
VCS: $1/[1+\Pi(Q^2)]$

Self-Energy, Unique to BH

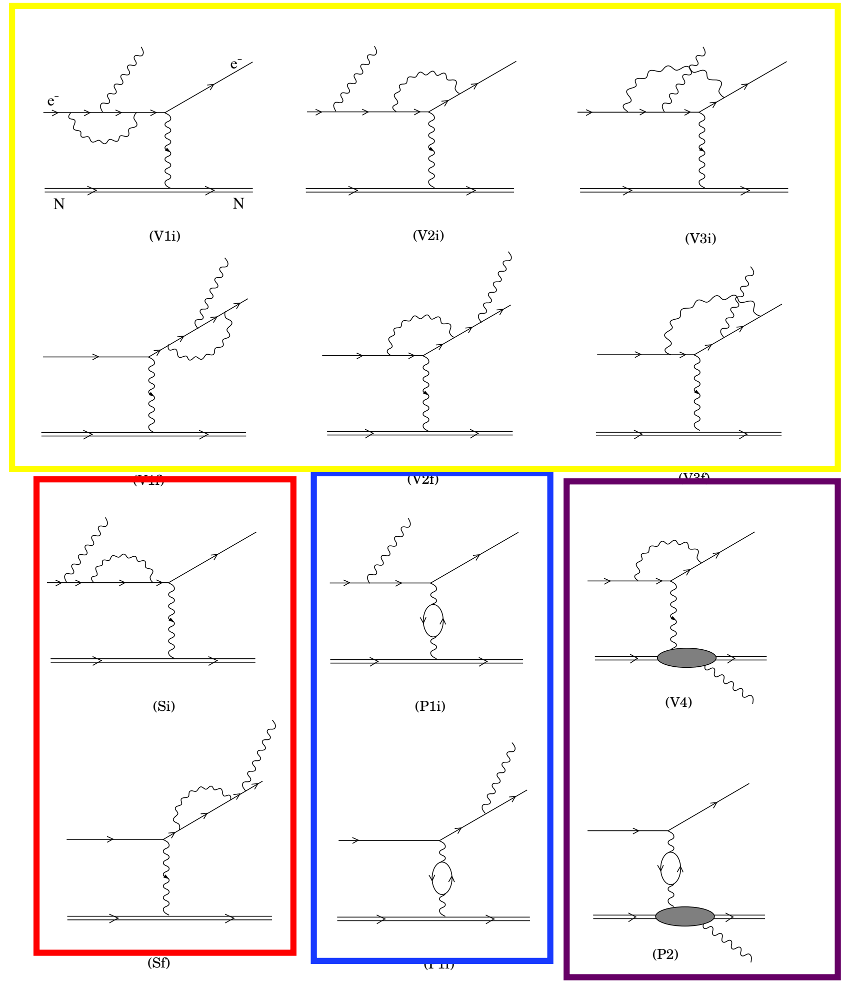

FIG. 2. First order virtual photon radiative corrections to the $ep \to ep\gamma$ reaction.

Real Radiative Corrections

Factorize in soft limit
Include lineshape in MC simulation.
Simulation and data are cut-off dependent (e.g. M_X^2 limit)

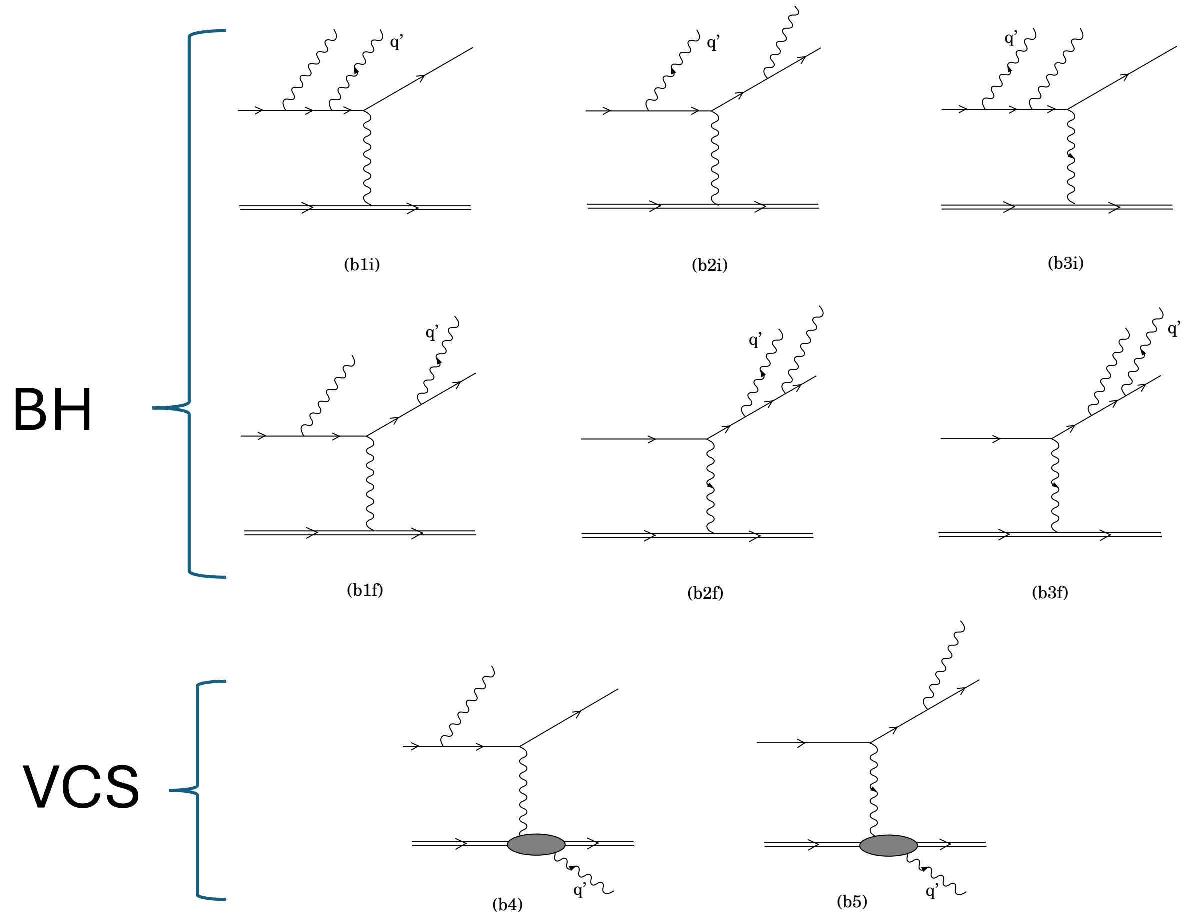

FIG. 3. First order soft photon emission contributions to the $ep \to ep\gamma$ reaction.

Correction to measured cross section to obtain "Born" cross section does not factorize

$$d\sigma = d\sigma^{\mathrm{VCS}} + d\sigma^{\mathrm{BH}} + \left[VCS^{\dagger} BH \right]$$

$$\Rightarrow d\sigma^{\mathrm{VCS}} \left[1 + \frac{\delta^{\mathrm{VCS}}_{\mathrm{vertex}} / 2}{1 - \Pi(Q^2)} \right]^2 + d\sigma^{\mathrm{BH}} \left[1 + \frac{\delta^{\mathrm{BH}}_{\mathrm{vertex}} / 2}{1 - \Pi(-t)} \right]^2 + \left[VCS^{\dagger} BH \right] \left[1 + \frac{\delta^{\mathrm{VCS}}_{\mathrm{vertex}} / 2}{1 - \Pi(Q^2)} \right] \left[1 + \frac{\delta^{\mathrm{BH}}_{\mathrm{vertex}} / 2}{1 - \Pi(-t)} \right]$$

- Model dependent calculation.
  - Hall A analysis uses P.Guichon code with old factorized GPD model
- Final correction is relatively insensitive to specific DVCS kinematics in JLab range.
  - ~10% effect